

RMF-BASED MICROSCOPIC STUDY OF GROUND-STATE PROPERTIES AND NUCLEAR SHAPE TRANSITIONS IN EVEN–EVEN Po ISOTOPES

VIRENDER THAKUR[†], PANKAJ KUMAR, VIKESH KUMAR
SMRITI THAKUR, ANUPRIYA SHARMA, RAJ KUMAR, SHASHI K. DHIMAN

Department of Physics, Himachal Pradesh University
Summer-Hill, Shimla-171005, India

*Received 23 October 2021, accepted 7 February 2022,
published online 23 February 2022*

Ground-state properties of even–even isotopes of polonium (Po) have been studied. The physical observables of our interest include quadrupole deformation and shape transitions, binding energies, charge radii, and neutron skin thickness. Theoretical results for the differential variation $dS_{2n}(Z, N)$ based on two-neutron separation energy are also presented. Theoretical calculations are carried out by employing covariant density functional theory with density-dependent meson exchange (DD-ME2) and point coupling (DD-PC1) interactions. The presented ground state properties with the RMF (Relativistic Mean Field) model are in good agreement with recently available experimental data. The theoretical estimates calculated by the covariant density functional theory predict shape transition from oblate to spherical and spherical to prolate along the isotopic chain of even–even Po nuclei ranging from mass number of 186 to 218.

DOI:10.5506/APhysPolB.53.2-A3

1. Introduction

A new phase of the research has begun with the development of experimental facilities like radioactive ion beams and other technological advancements [1–6]. The modern facilities make it possible to study a variety of the nuclides which are unexplored till now. One of the key problems in nuclear physics is the understanding of atomic nucleus due to the complexity of the many-body system. The study of neutron-rich nuclei is a wide-open area of the research in the nuclear structure field. The nuclei far away from the line of β stability is a matter of deep investigation and it is yet to be explored. The nuclei which are away from the β -stability line play an important role in the understanding of nuclear physics. The production of the new isotopes

[†] Corresponding author: virenthakur2154@gmail.com

[7–9] in recent years has revived great interest in nuclear structure models. Till today, very little information is available about those nuclei which are lying near driplines (exotic or halo nuclei).

The study of the nuclear structure properties near the drip lines and away from β -stability, especially for the heavy-mass range nuclei mainly depends upon the theoretical models since the experimental data is available only for the light nuclei and also the data available is not huge. The nuclear many-body system is a very complex system and an effective theoretical model is needed for the strong and reliable predictions for the nuclear structure systems. It is also true that the undiscovered nuclei that are stable and form a bound system are very large in number and we cannot study all of them, however, we are able to make an effective step by examining a few of them. We have chosen a heavy-mass-range isotopic chain of $^{186-218}\text{Po}$ for our theoretical study and the theoretical model is based on covariant DFT. The nuclear many-body dynamics can be understood very well by using the density functional theory both in relativistic and non-relativistic regimes [10–18]. The successes and applications of covariant DFT can be found in [14]. In our manuscript, the RHB (Relativistic Hartree–Bogoliubov) model [19] with density-dependent effective interactions of point-coupling-types (DD-PC1 [20]) and meson exchange (DD-ME2 [21]) is employed with the inclusion of separable pairing interaction [22–24]. The RHB theory has been tested several times and its successes involve the appreciable description of nuclei near the drip lines (exotic nuclides) [25, 26]. It has also been used to study the deformed exotic nuclides as reported in [27, 28]. Studies related to the shell structure and shell closure based on covariant DFT are also available in [12, 29]. All these studies make this theory really a promising one to investigate the many-body systems. In the presented work, the systematic constrained calculations for the potential energy curves (PECs) for the isotopic chain of $^{186-218}\text{Po}$ are presented. We have also theoretically calculated the results for other important ground-state properties such as systematics of binding energy, charge radii, neutron skin thickness, two-neutron separation energy, and shell closure parameter. The organisation of the presented paper is as follows. An overview of the RHB theory with employed effective interactions is presented in Section 2. In Section 3, the results of our theoretical calculations in comparison to the recent experimental data are presented. The presented work is summarized in Section 4.

2. Theoretical framework

The presented work is carried out with the RHB (Relativistic Hartree–Bogoliubov) theory. The theory describes a nucleus as a relativistic system of baryons and mesons, and the ground state of the system is described as a vacuum with respect to the independent quasiparticle operators, which

are defined by the unitary Bogoliubov transformation of the single nucleon creation and annihilation operators. The details of the RHB model are given in Refs. [21, 30]. We have employed the model based on the RHB theory with the density-dependent effective interactions. The density-dependent meson exchange and point coupling effective interactions are used to study the shell structure evolution. The pairing correlations are also taken into consideration by the RHB functional constructed through the Bogoliubov transformation of quasi-particle operators. This model is briefly discussed in the following subsections.

2.1. DD-ME model

In this model, the total Lagrangian [21] density can be written in the following form:

$$\begin{aligned}
 \mathcal{L} = & \sum_i \bar{\psi}_i (i\gamma_\mu \partial^\mu - m) \psi_i + \frac{1}{2} \partial_\mu \sigma \partial^\mu \sigma - \frac{1}{2} m_\sigma^2 \sigma^2 \\
 & - \frac{1}{2} \Omega_{\mu\nu} \Omega^{\mu\nu} + \frac{1}{2} m_\omega^2 \omega_\mu \omega^\mu - \frac{1}{4} \vec{R}_{\mu\nu} \vec{R}^{\mu\nu} + \frac{1}{2} m_\rho^2 \vec{\rho}_\mu \cdot \vec{\rho}^\mu \\
 & - \frac{1}{4} F_{\mu\nu} F^{\mu\nu} - g_\sigma \bar{\psi} \psi \sigma - g_\omega \bar{\psi} \gamma^\mu \psi \omega_\mu - g_\rho \bar{\psi} \vec{\tau} \gamma^\mu \psi \cdot \vec{\rho}_\mu \\
 & - e \bar{\psi} \gamma^\mu \psi A_\mu.
 \end{aligned} \tag{1}$$

In Eq. (1), ω represents isoscalar–vector meson, σ represents isoscalar–scalar meson, the term ρ refers to isovector–vector meson.

2.2. DD-PC model

In a complete analogous way to the meson-exchange RMF phenomenology described before, a density-dependent interaction Lagrangian density of point coupling models [20], which includes the isoscalar–vector $(\bar{\psi} \gamma_\mu \psi)(\bar{\psi} \gamma^\mu \psi)$, isoscalar–scalar $(\bar{\psi} \psi)^2$, and isovector–vector $(\bar{\psi} \vec{\tau} \gamma_\mu \psi) \cdot (\bar{\psi} \vec{\tau} \gamma^\mu \psi)$ four-fermion contact interactions in the isospace–space can be written as

$$\begin{aligned}
 \mathcal{L} = & \bar{\psi} (i\gamma \partial - m) \psi - \frac{1}{2} \alpha_S(\rho) (\bar{\psi} \psi) (\bar{\psi} \psi) \\
 & - \frac{1}{2} \alpha_V(\rho) (\bar{\psi} \gamma^\mu \psi) (\bar{\psi} \gamma_\mu \psi) - \frac{1}{2} \alpha_{TV}(\rho) (\bar{\psi} \vec{\tau} \gamma^\mu \psi) \cdot (\bar{\psi} \vec{\tau} \gamma_\mu \psi) \\
 & - \frac{1}{2} \delta_S (\partial_\nu \bar{\psi} \psi) (\partial^\nu \bar{\psi} \psi) - e \bar{\psi} \gamma A \frac{1 - \tau_3}{2} \psi.
 \end{aligned} \tag{2}$$

2.3. RHB approximation with a separable pairing interactions

The Relativistic Hartree–Bogoliubov model [31, 32] takes into account the pairing correlations in the RHB functional also in terms of the quasi-particle operators [33]. The pairing correlations are important to consider

for a quantitative description of an open-shell nuclei. The formulation of the RHB model is a relativistic extension of the conventional Hartree–Fock–Bogoliubov (HFB) framework in which the mean field and pairing correlations are treated self-consistently. The RHB model gives a unified description of particle–hole (ph) and particle–particle (pp) correlations on a mean-field level by using the average self-consistent mean-field potential that encloses the long-range ph correlations, and a pairing-field potential which sums up the pp correlations. The density matrix in the presence of pairing can be generalized to two densities, the normal density $\hat{\rho}$, and pairing tensor $\hat{\kappa}$. The Relativistic Hartree–Bogoliubov energy density functional can be written as

$$E_{\text{RHB}}[\hat{\rho}, \hat{\kappa}] = E_{\text{RMF}}[\hat{\rho}] + E_{\text{pair}}[\hat{\kappa}], \quad (3)$$

where $E_{\text{RMF}}[\hat{\rho}]$ is the nuclear energy density functional and is given by

$$E_{\text{RMF}}[\psi, \bar{\psi}, \sigma, \omega^\mu, \bar{\rho}^\mu, A^\mu] = \int d^3r \mathcal{H}(r). \quad (4)$$

The pairing part of RHB functional is given by

$$E_{\text{pair}}[\hat{\kappa}] = \frac{1}{4} \sum_{n_1 n'_1} \sum_{n_2 n'_2} \kappa_{n_1 n'_1}^* \langle n_1 n'_1 | V^{\text{PP}} | n_2 n'_2 \rangle \kappa_{n_2 n'_2}, \quad (5)$$

where $\langle n_1 n'_1 | V^{\text{PP}} | n_2 n'_2 \rangle$ are the matrix elements of the two-body pairing interaction and indices n_1, n'_1, n_2 , and n'_2 denote quantum numbers that specify the Dirac indices of the spinor.

The pairing force is separable in momentum space and in r-space has the form of

$$V^{\text{PP}}(r_1, r_2, r'_1, r'_2) = -G\delta(R - R') P(r)P(r'), \quad (6)$$

where $R = \frac{1}{\sqrt{2}}(r_1 + r_2)$ and $r = \frac{1}{\sqrt{2}}(r_1 - r_2)$ represent the center of mass and the relative coordinates, respectively, and the form factor $P(r)$ is of the Gaussian form written as

$$P(r) = \frac{1}{(4\pi a^2)^{3/2}} e^{-r^2/2a^2}. \quad (7)$$

The pairing force has a finite range and it also conserves translational invariance due to the presence of the factor $\delta(R - R')$. Finally, the pairing energy in the nuclear ground state is given by

$$E_{\text{pair}} = -G \sum_N P_N^* P_N. \quad (8)$$

The details can be found in Refs. [22, 34].

3. Results and discussions

We present our computed results of quadrupole deformation and shape transitions, binding Energies, charge radii, neutron skin thickness, two-neutron separation energies $S_{2n}(Z, N)$, and the differential variation of the two-neutron separation energy $dS_{2n}(Z, N)$ for the isotopic chain of polonium (Po) ranging from mass number of 186 to 218. The theoretical calculations are carried out within the framework of the RHB theory discussed briefly in the previous section.

3.1. Quadrupole deformation and shape transition

We have shown our results for the quadrupole deformation parameter and the shape transition for the even–even Po isotopes ranging from mass number $A = 186$ to $A = 218$ in Figs. 1, 2, 3, 4, and 5. The reason of interest for the shape transitions in nuclei is very obvious as it is the fundamental property of the nuclei. Nucleons try to adjust themselves inside the nuclei in such a manner so that the overall distribution is corresponding to the maximum possible binding energy. In the axially symmetric case, the deformed nuclei can exist in the prolate or oblate shape configuration. The positive value of the quadrupole deformation parameter (β_2) is corresponding to the prolate shape and the negative value of β_2 shows the oblate shape deformation. The Po isotopes belong to the heavy-mass region and in Ref. [35], there is no sign of substantial triaxiality involved in the case of Po isotopes. This is why we have considered the axial shapes in our study.

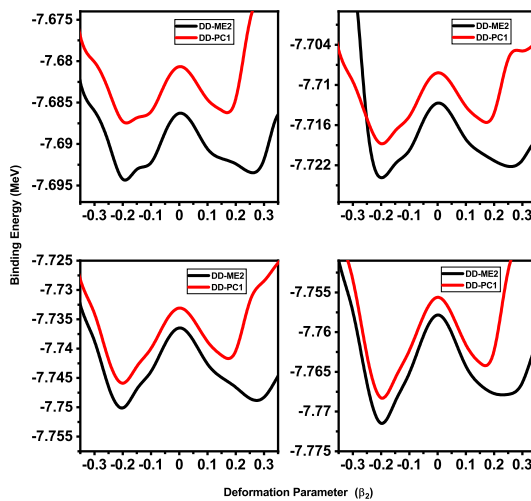


Fig. 1. The potential energy curves (PEC) plotted as a function of β_2 for the $^{186-192}\text{Po}$ isotopes. The theoretical estimates are computed by using the relativistic nuclear density functional based on the DD-ME2 and DD-PC1 parameters.

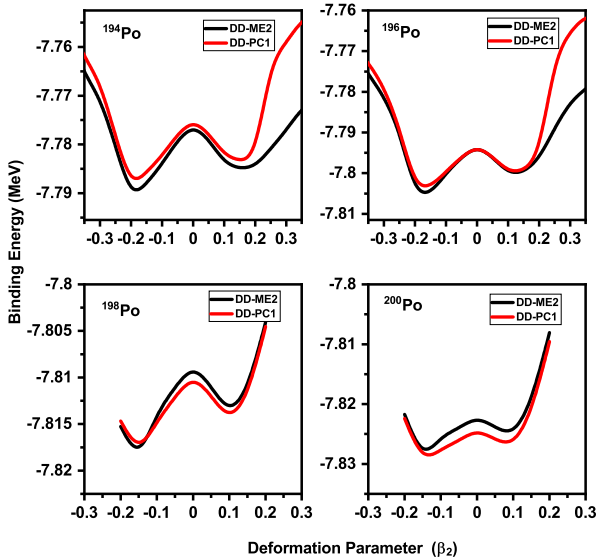


Fig. 2. The potential energy curves (PEC) plotted as a function of β_2 for the $^{194-200}\text{Po}$ isotopes. The theoretical estimates are computed by using the relativistic nuclear density functional based on the DD-ME2 and DD-PC1 parameters.

The potential energy curves (PECs) are shown in Figs 1, 2, 3, 4, and 5 for the isotopic chain of the polonium nuclei $^{186-218}\text{Po}$. The most stable configuration corresponding to the deformation parameter is the one where the binding energy per nucleon value is most negative. The negative value here indicates that this much of additional energy is required to disassemble the nucleon from the respective nuclei and that is why it is called the binding energy per nucleon. The theoretical estimates are computed by using the relativistic nuclear density functional based on the DD-ME2 and DD-PC1 parameters. From the PECs drawn in Figs. 1, 2, 3, 4, and 5, it can be easily extracted that there is a shape transition from oblate to spherical and then spherical to oblate as one moves from ^{186}Po to ^{218}Po . Isotopes ranging from ^{186}Po to ^{204}Po show the oblate-shape configuration and ^{206}Po to ^{214}Po correspond to the spherical shape and, afterward, there is a transition to prolate-shape configuration for the ^{216}Po and ^{218}Po nuclides. It can be easily seen that the nuclei near the magic number of neutron $N = 126$ are spherical and the isotopes close to $N = 126$ show either none or slight deformation from the spherical symmetry. This fact is attributed to the magicity of the neutron number $N = 126$ and as one moves away from this configuration along the isotopic chain, the redistribution of the nucleons among the nuclei leads to the deformation in order to get the state of maximum stability in that particular configuration of the nucleons.

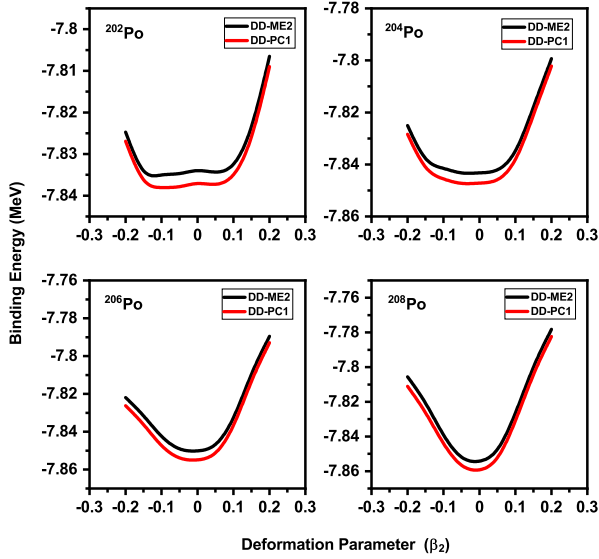


Fig. 3. The potential energy curves (PEC) plotted as a function of β_2 for the $^{202-208}\text{Po}$ isotopes. The theoretical estimates are computed by using the relativistic nuclear density functional based on the DD-ME2 and DD-PC1 parameters.

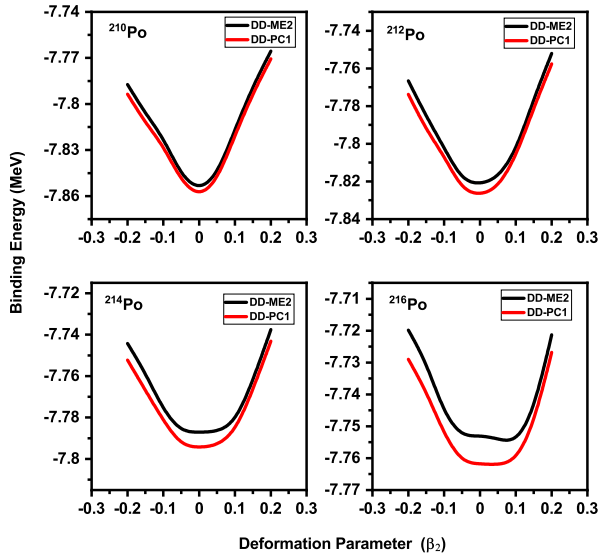


Fig. 4. The potential energy curves (PEC) plotted as a function of β_2 for the $^{210-216}\text{Po}$ isotopes. The theoretical estimates are computed by using the relativistic nuclear density functional based on the DD-ME2 and DD-PC1 parameters.

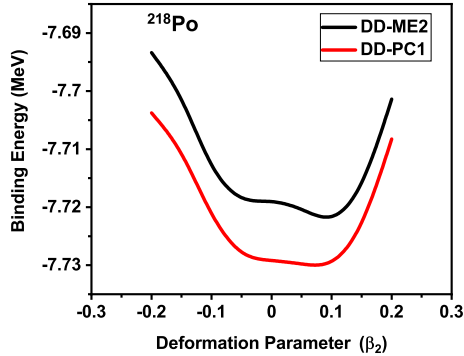


Fig. 5. The potential energy curves (PEC) plotted as a function of β_2 for the ^{218}Po isotope. The theoretical estimates are computed by using the relativistic nuclear density functional based on the DD-ME2 and DD-PC1 parameters.

3.2. Binding energy and its derived physical observables

Binding energy is the underlying property of the nuclides which provides the deep insights into the nuclear structure. The binding energy refers to that energy which when given to the nuclei, breaks it apart into its constituent nucleons. The binding energy is directly related to the stability of the nuclei. The quantities such as nuclear separation energy, shell closure parameters which are also the important observables related to the nuclei can be calculated using the binding energy. The theoretical results of the binding energy per nucleon for the isotopic chain of polonium isotopes are shown in Fig. 6. The theoretical extractions based on the RHB theory are compared with the available experimental data taken from Ref. [36] and they are in

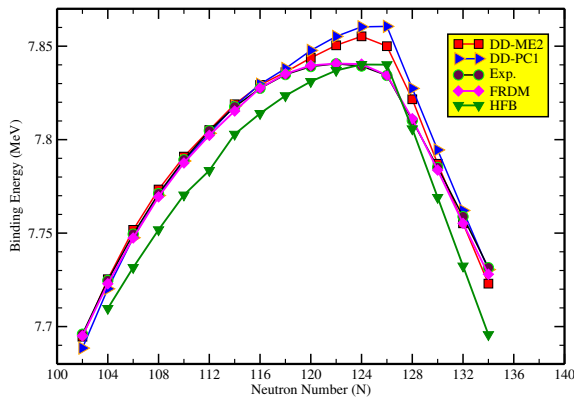


Fig. 6. Variation of theoretical and experimental [36] binding energies (BE) as a function of neutron number (N) for the $^{186}\text{-}^{218}\text{Po}$ isotopes. Data taken from the FRDM [37] and HFB [35] calculations is also shown for comparison.

good agreement with the experimental extractions. We have also compared our results with the calculations obtained from the Finite Range Droplet model (FRDM) [37] and the Hartree–Fock–Bogoliubov (HFB) model [35] which are also in agreement with our results. It can be observed from Fig. 6 that the binding energy per nucleon increases from neutron number $N = 102$ to $N = 124$, and after that, there is a decrease in the binding energy up to the neutron number of $N = 134$. The present systematics of binding energy per nucleon indicates that as we add more and more neutrons to the nuclei, the stability gets increased as the excess of neutron overcomes the Coulomb repulsion among the protons up to the neutron number near the magic shell neutron number $N = 126$. After that, there is a decreasing trend in binding energy per nucleon attributed to the fact that the asymmetry between the proton and the neutron number gets increased and this reduces the stability.

Figures 7 and 8 show the theoretical results for the physical observables derived from the binding energies, and these physical observables are two-neutron separation energy S_{2n} and the shell closure parameter dS_{2n} based on the two-neutron separation energy. The two-neutron separation energy gives the measure of the energy that is essentially required to remove two neutrons from a particular nucleus. It is defined by using the formula

$$S_{2n}(Z, N) = [B(Z, N) - B(Z, N - 2)]. \quad (9)$$

The authors in Ref. [38] have proposed an important physical quantity

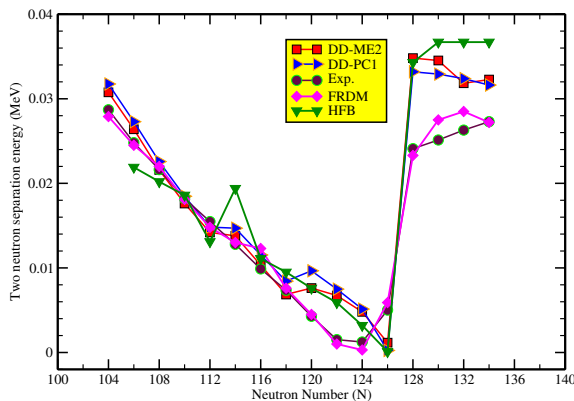


Fig. 7. Theoretically calculated two-neutron separation energy (S_{2n}) of the even–even $^{186-218}\text{Po}$ isotopes and its comparison with experimental data [36] as a function of neutron number (N). The theoretical estimates are computed by using the relativistic nuclear density functional based on the DD-ME2 and DD-PC1 parameters. Data taken from the FRDM [37] and HFB [35] calculations is also shown for comparison.

$dS_{2n}(Z, N)$ based on two-neutron separation energies which is used to identify the appearance or the collapse of the shell closures. It is defined by using the formula

$$dS_{2n}(Z, N) = \left| \frac{S_{2n}(Z, N + 2) - S_{2n}(Z, N)}{2} \right|. \quad (10)$$

We have theoretically calculated the results of $S_{2n}(Z, N)$ and $dS_{2n}(Z, N)$ for the even-even isotopes of polonium (Po) in Figs. 7 and 8, respectively, and plotted them against the neutron number (N). We have also compared our theoretical results with the available experimental data [36] and with the calculations obtained from the FRDM [37] and HFB [35] models. It can be seen in Fig. 7 that there is a substantial drop in $S_{2n}(Z, N)$ values across ^{210}Po indicating the neutron number $N = 126$ as the neutron shell closure in the isotopic chain of even-even Po nuclides. The presence of the shell closure at $N = 126$ in ^{210}Po is also supported in the Fig. 8 where we presented the variation of $dS_{2n}(Z, N)$ values for the isotopic chain of Po. A peak is observed at neutron number $N = 126$ indicating a shell gap. The theoretical estimates are computed by using the relativistic nuclear density functional based on the DD-ME2 and DD-PC1 parameters.

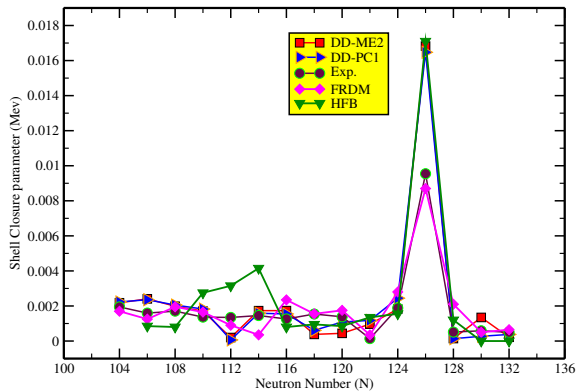


Fig. 8. Theoretically calculated differential shell closure parameter (dS_{2n}) of the even-even $^{186-218}\text{Po}$ isotopes and its comparison with experimental data [36] as a function of neutron number (N). The theoretical estimates are computed by using the relativistic nuclear density functional based on the DD-ME2 and DD-PC1 parameters. Data taken from the FRDM [37] and HFB [35] calculations is also shown for comparison.

3.3. Charge radii

The nuclear charge radius is the fundamental nuclear observable that estimates the size of the nucleus. In this subsection, we are presenting the results of nuclear charge radii which is evaluated using different interactions such as DD-ME2 and DD-PC1 with covariant DFT. Figure 9 presents our theoretical results of root-mean-square charge radii. The results for the charge radii R_{ch} in the Fermi meter as a function of neutron number N for the isotopic chain of even–even Po are shown. The theoretical charge radius is calculated using the formula [22]

$$R_{\text{ch}} = \sqrt{r_p^2 + 0.64} \text{ fm}. \quad (11)$$

Here, r_p denotes the r.m.s. radius of the proton density distribution and term 0.64 fm^2 accounts for the finite size of the proton.

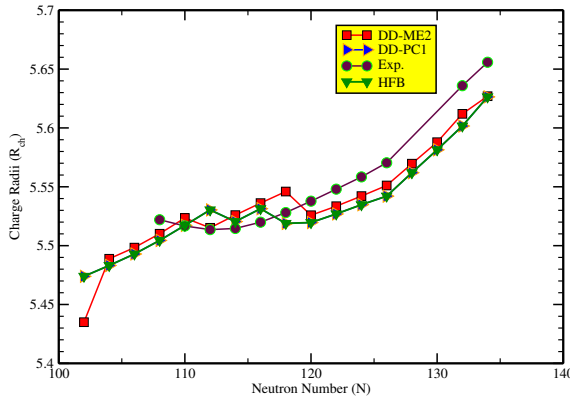


Fig. 9. Comparison of experimental [39] and theoretically calculated root-mean-square charge radii (R_{ch}) plotted against the neutron number (N) for the even–even $^{186-218}\text{Po}$ isotopes. The theoretical estimates are computed by using the relativistic nuclear density functional based on the DD-ME2 and DD-PC1 parameters. Data taken from the HFB [35] calculations is also shown for comparison.

The experimental measurements of R_{ch} are also shown for comparison [39]. The experimentally observed systematics of charge radii is very well reproduced by our theoretical calculations based on the RMF model with covariant DFT. We have also compared our results with those obtained from the HFB model [35] which are also in agreement with our results and follow a similar trend as our results. It is clear from Fig. 9 that, as the neutron number N increases for the isotopic chain of the even–even Po isotopes, there is an increase in the charge radii and it keeps on increasing. This trend is attributed to a redistribution of the nucleons inside the nuclei to overcome the Coulomb repulsion by the addition of an excess of the neutron.

3.4. Neutron skin thickness

The neutron skin thickness Δr_{np} is defined by the following equation:

$$\Delta r_{np} = \sqrt{r_n^2} - \sqrt{r_p^2}, \quad (12)$$

where r_n refers to the neutron r.m.s. radius and r_p denotes the proton r.m.s. radius. It is well-understood from Ref. [40] that the accurate measurement of the neutron skin thickness would place rigid constraints on the density dependence of the nuclear symmetry energy denoted as $S(\rho)$. The density dependence of the nuclear symmetry energy has direct consequences in finite nuclear matter and nuclear dense matter of astrophysical interest. This makes this nuclear observable a very important one that can reveal many insights about the nuclei. Within the available experimental technology in nuclear physics, the nuclear symmetry energy cannot be measured directly but the information of this fundamental quantity can be extracted from the neutron skin thickness and electric dipole polarizability [41]. In Fig. 10, we present the neutron skin thickness $\Delta r_{np} = r_n - r_p$ in fm, plotted as a function of neutron number N for the chain of even-even Po isotopes. The theoretical estimates are computed by using the relativistic nuclear density functional based on the DD-ME2 and DD-PC1 parameters. We have also compared our results with the results obtained from the HFB model [35]. It can be seen from Fig. 10 that the magnitudes of skin thickness are increasing systematically with an increase in the neutron number along the isotopic

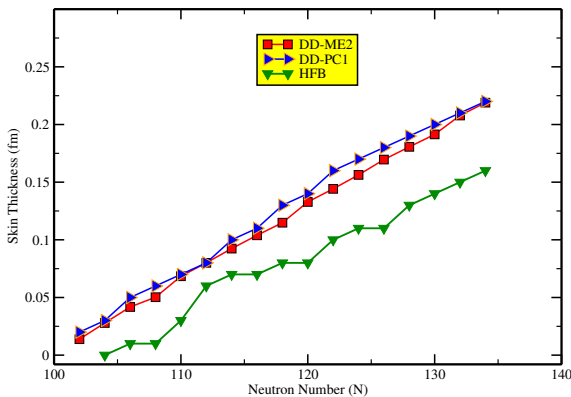


Fig. 10. The neutron skin thickness (Δr_{np}) of the even-even $^{186-218}\text{Po}$ isotopes plotted against the neutron number (N). The theoretical estimates are computed by using the relativistic nuclear density functional based on the DD-ME2 and DD-PC1 parameters. Data taken from the HFB [35] calculations is also shown for comparison.

chain of even–even Po nuclides. This gradual increase in the neutron skin may be attributed to the redistribution of the nucleons as a result of nuclear interactions with the addition of extra neutrons keeping the atomic number (Z) fixed up to the neutron drip line.

4. Conclusions

We have got some of the very important conclusions based upon our theoretical estimations presented in this paper by employing Nuclear Density Functionals based on the Relativistic Hartree–Bogoliubov (RHB) with the different effective interactions such as DD-PC1 and DD-ME2. The systematics of average binding energy, two-neutron separation energy, shell closure parameter, nuclear charge radii, and neutron skin thickness have been calculated and compared with the available experimental data. The theoretically calculated results are in good agreement with the experimental data and also predict the values of observables for which experimental data is not available. We have also compared our results with the results obtained from the FRDM [37] and HFB [35] models which are also in agreement with our results. The present theoretical results of nuclear structure properties support the existence of shell closure at $N = 126$. The results for quadrupole deformation and potential energy curves indicate the shape transition from oblate to spherical and spherical to prolate along the isotopic chain of Po nuclei ranging from mass number of 186 to 218.

Virender Thakur is highly thankful to Himachal Pradesh University (HPU) for giving access to the computational facilities and DST-INSPIRE (Govt. of India) for providing financial support (JRF/SRF scheme). The Authors would like to express deep gratitude to Prof. Peter Ring for fruitful discussion. Authors would also like to thank the anonymous referee(s) for the thorough inspection of the presented manuscript and valuable comments.

REFERENCES

- [1] A. Gade *et al.*, «In-Beam γ -Ray Spectroscopy of Very Neutron-Rich Nuclei: Excited States in ^{46}S and ^{48}Ar », *Phys. Rev. Lett.* **102**, 182502 (2009).
- [2] E. Lunderberg *et al.*, «In-beam γ -ray spectroscopy of $^{38-42}\text{S}$ », *Phys. Rev. C* **94**, 064327 (2016).
- [3] T. Motobayashi, «World new facilities for radioactive isotope beams», *EPJ Web Conf.* **66**, 01013 (2014).
- [4] M.A. Famiano, «Nuclear mass measurements with radioactive ion beams», *Int. J. Mod. Phys. E* **28**, 1930005 (2019).

- [5] J.C. Yang *et al.*, «High Intensity heavy ion Accelerator Facility (HIAF) in China», *Nucl. Instrum. Methods Phys. Res. B* **317**, 263 (2013).
- [6] D. Jeon *et al.*, «Design of the RAON accelerator systems», *J. Korean Phys. Soc.* **65**, 1010 (2014).
- [7] S. Bhattacharyya *et al.*, «Structure of Neutron-Rich Ar Isotopes Beyond $N = 28$ », *Phys. Rev. Lett.* **101**, 032501 (2008).
- [8] O.V. Bernalova *et al.*, «Evolution of single-particle structure of silicon isotopes», *Eur. Phys. J. A* **54**, 2 (2018).
- [9] F. Nowacki, A. Obertelli, A. Poves, «The neutron-rich edge of the nuclear landscape: Experiment and theory», *Prog. Part. Nucl. Phys.* **120**, 103866 (2021), [arXiv:2104.06238 \[nucl-th\]](#).
- [10] P. Ring, «Relativistic mean field theory in finite nuclei», *Prog. Part. Nucl. Phys.* **37**, 193 (1996).
- [11] J. Meng (Ed.) «Relativistic Density Functional for Nuclear Structure. International Review of Nuclear Physics Vol. 10», *World Scientific, Singapore* 2016.
- [12] L.S. Geng, H. Toki, J. Meng, «A systematic study of neutron magic nuclei with $N = 8, 20, 28, 50, 82$ and 126 in the relativistic mean-field theory», *J. Phys. G: Nucl. Part. Phys.* **30**, 1915 (2004).
- [13] S.E. Agbemava, A.V. Afanasjev, D. Ray, P. Ring, «Global performance of covariant energy density functionals: Ground state observables of even-even nuclei and the estimate of theoretical uncertainties», *Phys. Rev. C* **89**, 054320 (2014).
- [14] P.-W. Zhao *et al.*, «New parametrization for the nuclear covariant energy density functional with a point-coupling interaction», *Phys. Rev. C* **82**, 054319 (2010).
- [15] V. Thakur, S.K. Dhiman, «A study of charge radii and neutron skin thickness near nuclear drip lines», *Nucl. Phys. A* **992**, 121623 (2019).
- [16] V. Thakur *et al.*, «Microscopic study of the shell structure evolution in isotopes of light to middle mass range nuclides», *Nucl. Phys. A* **1002**, 121981 (2020), [arXiv:2001.10215 \[nucl-th\]](#).
- [17] P. Kumar, S.K. Dhiman, «Microscopic study of shape evolution and ground state properties in even-even Cd isotopes using covariant density functional theory», *Nucl. Phys. A* **1001**, 121935 (2020).
- [18] P. Kumar *et al.*, «Nuclear shape evolution and shape coexistence in Zr and Mo isotopes», *Eur. Phys. J. A* **57**, 36 (2021), [arXiv:2007.07479 \[nucl-th\]](#).
- [19] H. Kucharek, P. Ring, «Relativistic field theory of superfluidity in nuclei», *Z. Physik A* **339**, 23 (1991).
- [20] T. Nikšić, D. Vretenar, P. Ring, «Relativistic nuclear energy density functionals: Adjusting parameters to binding energies», *Phys. Rev. C* **78**, 034318 (2008).

- [21] G.A. Lalazissis, T. Nikšić, D. Vretenar, P. Ring, «New relativistic mean-field interaction with density-dependent meson–nucleon couplings», *Phys. Rev. C* **71**, 024312 (2005).
- [22] T. Nikšić, N. Paar, D. Vretenar, P. Ring, «DIRHB — A relativistic self-consistent mean-field framework for atomic nuclei», *Comput. Phys. Commun.* **185**, 1808 (2014).
- [23] T. Nikšić *et al.*, «3D relativistic Hartree–Bogoliubov model with a separable pairing interaction: Triaxial ground-state shapes», *Phys. Rev. C* **81**, 054318 (2010).
- [24] Y. Tian, Z.Y. Ma, P. Ring, «A finite range pairing force for density functional theory in superfluid nuclei», *Phys. Lett. B* **676**, 44 (2009).
- [25] J. Meng, P. Ring, «Relativistic Hartree–Bogoliubov Description of the Neutron Halo in ^{11}Li », *Phys. Rev. Lett.* **77**, 3963 (1996).
- [26] L.S. Geng, H. Toki, A. Ozawa, J. Meng, «Proton and neutron skins of light nuclei within the relativistic mean field theory», *Nucl. Phys. A* **730**, 80 (2004).
- [27] S.-G. Zhou *et al.*, «Neutron halo in deformed nuclei», *Phys. Rev. C* **82**, 011301 (2010).
- [28] L. Li *et al.*, «Deformed relativistic Hartree–Bogoliubov theory in continuum», *Phys. Rev. C* **85**, 024312 (2012).
- [29] W. Zhang *et al.*, «Magic numbers for superheavy nuclei in relativistic continuum Hartree–Bogoliubov theory», *Nucl. Phys. A* **753**, 106 (2005).
- [30] T. Nikšić, D. Vretenar, P. Ring, «Relativistic nuclear energy density functionals: Mean-field and beyond», *Prog. Part. Nucl. Phys.* **66**, 519 (2011).
- [31] D. Vretenar, A.V. Afanasjev, G.A. Lalazissis, P. Ring, «Relativistic Hartree–Bogoliubov theory: static and dynamic aspects of exotic nuclear structure», *Phys. Rep.* **409**, 101 (2005).
- [32] J. Meng *et al.*, «Relativistic continuum Hartree Bogoliubov theory for ground-state properties of exotic nuclei», *Prog. Part. Nucl. Phys.* **57**, 470 (2006).
- [33] P. Ring, Y.K. Gambhir, G.A. Lalazissis, «Computer program for the relativistic mean field description of the ground state properties of even–even axially deformed nuclei», *Comput. Phys. Commun.* **105**, 77 (1997).
- [34] T. Gonzalez-Llarena, J.L. Egido, G.A. Lalazissis, P. Ring, «Relativistic Hartree–Bogoliubov calculations with finite range pairing forces», *Phys. Lett. B* **379**, 13 (1996).
- [35] J.-P. Delaroche *et al.*, «Structure of even–even nuclei using a mapped collective Hamiltonian and the D1S Gogny interaction», *Phys. Rev. C* **81**, 014303 (2010).
- [36] M. Wang *et al.*, «The AME2016 atomic mass evaluation (II). Tables, graphs and references», *Chin. Phys. C* **41**, 030003 (2017).

- [37] P. Möller, A.J. Sierk, T. Ichikawa, H. Sagawa, «Nuclear ground-state masses and deformations: FRDM (2012)», *At. Data Nucl. Data Tables* **109–110**, 1 (2016).
- [38] M. Bhuyan, «Structural evolution in transitional nuclei of mass $82 \leq A \leq 132$ », *Phys. Rev. C* **92**, 034323 (2015).
- [39] I. Angeli, K.P. Marinova, «Table of experimental nuclear ground state charge radii: An update», *At. Data Nucl. Data Tables* **99**, 69 (2013).
- [40] B.K. Agrawal, S.K. Dhiman, R. Kumar, «Exploring the extended density-dependent skyrme effective forces for normal and isospin-rich nuclei to neutron stars», *Phys. Rev. C* **73**, 034319 (2006).
- [41] P.G. Reinhard, W. Nazarewicz, «Information content of a new observable: The case of the nuclear neutron skin», *Phys. Rev. C* **81**, 051303 (2010).